Nuclear polarization of Nd in the pseudocubic perovskite $NdAlO_3$ studied by neutron diffraction below 1 K

Elías Palacios,* Juan Bartolomé, and Fernando Luis
Instituto de Ciencia de Materiales de Aragón, CSIC-Universidad de Zaragoza, Pedro Cerbuna 13, 50009 Zaragoza, Spain

Rainer Sonntag
BENSC, Hahn-Meitner-Institut, Glienicker Strasse 100, D-14109 Berlin (Wannsee), Germany

(Received 3 July 2003; revised manuscript received 25 September 2003; published 24 December 2003)

Neutron-diffraction patterns collected on a powder sample of $NdAlO_3$ at 1.035 K and 500 mK and on a twinned crystal at 50 mK$<T<$1 K show an antiferromagnetic structure with the Nd^{3+} moments perpendicular to the trigonal axis of the crystal structure (rhombohedrally distorted perovskite, $R\bar{3}c, Z=6$). We obtain a magnetic moment $m=(1\pm0.1)\mu_B$. Below 200 mK a gradual increase of the magnetic lines is observed, attributed to the progressive polarization of the nuclear-spin ^{143}Nd and ^{145}Nd isotopes by the electronic magnetic hyperfine field B_{hf}. We obtain $B_{hf}=66\pm10$ T. Comparison with other compounds shows that the hyperfine field is proportional to the magnetic moment, consistently with the previously reported ratio, $B_{hf}/m=108$ T/μ_B for the orthorhombic perovskites.

DOI: 10.1103/PhysRevB.68.224425 PACS number(s): 75.30.Cr, 61.12.Bt, 61.12.Ld, 75.50.Ee

I. INTRODUCTION

The polarization of nuclear spins by a magnetic field appears at extremely low temperatures. Therefore, it is very difficult to study this phenomenon by neutron diffraction because of the unusually sophisticated device required to achieve the thermal shielding, and also due to the weak nuclear magnetic moment as compared to the usual electronic values. The ^{143}Nd and ^{145}Nd isotopes are two rare cases, since their scattering lengths for thermal neutrons strongly depend on the nuclear spin state, giving a large incoherent scattering cross section when the nuclear spin states are evenly populated. The coherent and incoherent scattering lengths for thermal neutrons are, respectively, $b_c=14.2(5)$ fm, $b_{inc}=21.1(6)$ fm for ^{143}Nd, and $b_c=14.2(5)$ fm, $b_{inc}=13(7)$ for ^{143}Nd.[1] This incoherent scattering would disappear at very low temperatures if the nuclear spins are polarized by a strong magnetic field either external or created by the electronic moment, i.e., hyperfine field. In the latter case, the spatial periodicity of the magnetically ordered nuclei in a solid is the same as that of the electronic magnetic moment causing its polarization. Therefore the incoherent scattering becomes coherent, thus increasing the intensity of the standard magnetic Bragg reflections. This has been called ''hyperfine-enhanced nuclear polarization's (HENP), of the Nd nucleus.[2]

The effect has been observed in several Nd compounds with different magnetic structures such as $NdPd_3$,[3] Nd_2CuO_4,[4] $NdGaO_3$,[2] $NdScO_3$,[5] and $NdFeO_3$.[6] In the first two cases it is superimposed to rather complex magnetic structures, making the problem difficult to study. The three latter compounds belong to the family of distorted perovskites, with simpler crystal and magnetic structures. The $NdMO_3$ (M being a trivalent ion) compounds are exciting since the ground state of the Nd atom is determined by the electric crystal field, which in turn depends on the symmetry and distances to the nearest ions, and on the exchange constants, being different for each particular compound. As a consequence, the electronic magnetic moment m varies over a wide range of values from about $1\mu_B$ to that of the free ion, $3.27\mu_B$. Thus these compounds enable us to study how HENP depends on m. There are several types of magnetic structures in this family. Using the Bertaut notation[7] for the Nd sublattice, these are classified as c_z for $NdCrO_3$, $NdCoO_3$, and $NdGaO_3$, or g_ya_x for $NdScO_3$ and $NdInO_3$, or c_yf_x for $NdFeO_3$. Most of these compounds have been studied on powder samples with the inherent problem of overlapping peaks and low intensity to background ratio.

A linear dependence of the hyperfine field with the electronic moment, $B_{hf}=Km$, with $K\cong108\pm2$T/μ_B was proposed,[8] but based on data obtained for $NdCrO_3$, $NdFeO_3$, and some intermetallic compounds only. In this paper we review the existing data for pseudocubic perovskites of orthorhombic structure, in a comprehensive way.

The $NdAlO_3$ is another interesting member of the family of distorted perovskites since it has a different crystal structure,[9,10] in which the Nd is the sole magnetic ion. The available crystals, sized of ~1 mm, are adequate to study by neutron diffraction. The crystal structure of $NdAlO_3$ derives from the cubic perovskite turning the AlO_6 octahedra by 10° around one of the ternary axes of the cubic unit cell. As a consequence, the symmetry is rhombohedral $R\bar{3}c$, with $Z=6$ in the hexagonal unit cell choice (Fig. 1). The crystals grow with faces perpendicular to the pseudocubic perovskite cell axes. There are four kinds of microtwins, each one choosing one of the threefold axes of the cubic cell as trigonal axis for the true rhombohedral symmetry. Because of this, frequent reference to the pseudocubic frame will be made throughout this paper. Figure 1 shows the relative position of the base vectors for the pseudocubic, rhombohedral, and rhombohedral referred to hexagonal (obverse) axes. Let us denote the indeices of a Bragg reflection, a crystal plane, or direction with a subscript C, R, or H when referred to the

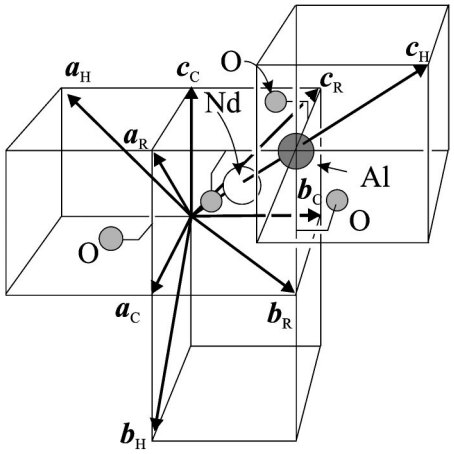

FIG. 1. Scheme of the crystal structure of $NdAlO_3$, showing some pseudocubic perovskite unit cells and the most representative atoms around a Nd site. The unit cell axes for different choices are also depicted: $(\mathbf{a}_c,\mathbf{b}_c,\mathbf{c}_c)$ for cubic, $(\mathbf{a}_R,\mathbf{b}_R,\mathbf{c}_R)$ for the primitive rhombohedral, and $(\mathbf{a}_H,\mathbf{b}_H,\mathbf{c}_H)$ for the hexagonal description of the rhombohedral lattice. The displacement of the O atoms with respect to their position in an ideal cubic perovskite structure are represented by small strokes.

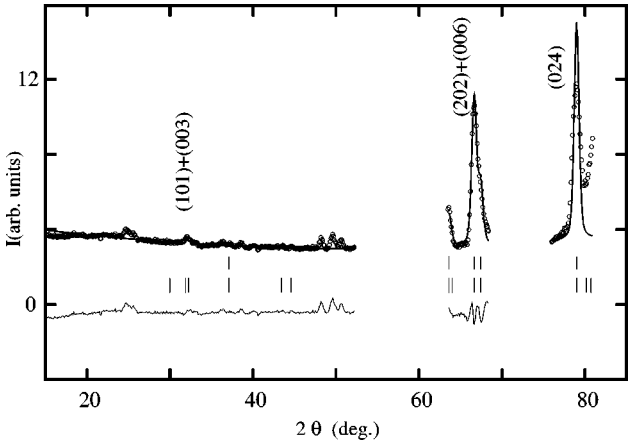

FIG. 2. Experimental (circles), calculated (line), and difference (lower line) powder neutron-diffraction patterns at 500 mK. The upper row of ticks shows the position of the nuclear Bragg peaks allowed for the $R\bar{3}c$ space group. The zero of the y scale does not hold for the difference pattern. The lower row indicates the position of the magnetic lines for all possible ordering modes with the same spatial periodicity as the nuclear structure. Some of them are labeled with respect to the hexagonal description of the rhombohedral unit cell. The (111) and (002) reflections coming from the aluminum of several layers of thermal shielding, which lie in the ranges $52.3°<2\theta<63.6°$ and $68.6°<2\theta<76°$, and the (111) and (002) reflections of the copper sample holder (at 69.6° and 82.5°, respectively) have been excluded. There are some peaks at about $2\theta=50°$ produced by the $\lambda/2$ harmonic, corresponding to the (022) reflection of Al and also an unidentified peak at 25°, already present at 1 K. The continuous line is a calculated pattern for the antiferromagnetic ordering with $m=0.9\mu_B$.

pseudocubic, rhombohedral, or hexagonal axes, for instance $(hkl)_C$.

Previous low-temperature (LT) heat-capacity (C_p) data showed a phase transition at $T_N=0.93\pm0.01$ K, which was then attributed to a possible antiferromagnetic ordering of the Nd^{3+} magnetic moments.[11] The entropy and the shape of the observed anomaly suggested a two-dimensional Ising system with $S=1/2$. In this work we focus on the determination of the magnetic structure and the HENP of Nd in this compound, by neutron diffraction in the temperature range 50 mK $<T<2$ K, on powder and crystal samples. Theoretical expressions for HENP in a twinned crystal will also be obtained (in the Appendix) and applied to $NdAlO_3$. The hyperfine field B_{hf} found and the magnetic Nd moment m are compared to available data for other Nd compounds, and a general rule connecting both magnitudes is deduced.

II. POWDER NEUTRON DIFFRACTION

The diffraction data were collected at the E6 diffractometer[12] of the BENSC in the Hahn-Meitner Institute (Berlin). Temperatures down to 50 mK were achieved using a ^{3}He/^{4}He dilution refrigerator coupled to an standard ILL He gas flow device. The thermal neutron beam was monochromated by a set of focusing PG crystals using the (002) Bragg reflection of graphite, giving $\lambda=2.38$ Å. The contribution of the first harmonic with $\lambda/2$ was reduced using a graphite filter to about a thousandth of the intensity in the monochromated beam.

The experiment was carried out on 0.5 g of $NdAlO_3$ mounted on a copper vessel attached to the mixing chamber of the dilution cryostat. In order to improve the thermal contact between sample and mixing chamber, a small amount of ^{3}He exchange gas was introduced in the sample holder, which proved to be effective down to about 200 mK. The diffraction pattern was collected using a multidetector of BF_3, with 200 channels of 0.1° width each. The data were taken in steps covering the angular range $14.5°<2\theta<82.4°$, at temperatures $T=1$ K and 500 mK, that is, above the transition, and well below it, respectively. Figure 2 shows the pattern measured at 500 mK together with the position of the nuclear and magnetic Bragg peaks. In addition to the Bragg reflections coming from the sample there are also present some peaks of much stronger intensity coming from the sample holder (copper) and from the several aluminum layers which act as thermal shielding. Therefore the range $52.3°<2\theta<63.5°$ was not measured and data in the range $68.6°<2\theta<76°$ were excluded from the plot and not taken into account in the subsequent analysis. There are also some peaks in the range $2\theta<52°$ coming from the sample holder and shielding which are produced by the $\lambda/2$ harmonic of the incoming radiation. Finally there is an unexplained peak about $2\theta=25°$ which is present above 1 K and probably comes from some unidentified part of the cryostat.

The magnetic contribution to diffraction is revealed by the difference between the patterns taken at 500 mK and at 1 K. In the accessible range of measurement this difference shows only a resolvable peak at $2\theta\cong32°$, which can be indexed as $(\frac{1}{2},\frac{1}{2},\frac{1}{2})_C$. It indicates purely antiferromagnetic order in which each Nd moment is antiparallel to its nearest neighbors. The magnetic moment m can be deduced from the rela-

tive intensity of the magnetic peak with respect to the pure nuclear ones in the original pattern, which can be easily computed for the known crystal structure. The pattern calculated for $m=0.9\mu_B$ is compared in Fig. 2 to the experimental data. It fits properly the intensity of the reflection $(111)_C=(202)_H+(006)_H$. Adjusting the scale factor to fit the other observed nuclear reflection, $(200)_C=(024)_H$, would give $m=1.1\mu_B$. Thus a resulting value $m=(1.0\pm0.1)\mu_B$ can be given, the uncertainty due to the two different values obtained when using the first or the second reflection as scaling datum. The antiferromagnetic character of the ordering agrees with the shape of the LT limit of the λ peak (proportional to T^3) observed in the heat-capacity data.[11] The obtained value for m agrees with the expected result from crystal-field calculations, based on the higher temperature susceptibility and Raman spectrum, which gave $g=1.81$, or $m=0.91\mu_B$, for the lowest doublet of the ground state.[13]

III. DIFFRACTION ON A TWINNED CRYSTAL

The experiments were carried out on the two axis diffractometer E4 of the BENSC with unpolarized thermal neutrons monochromated by a set of PG crystals selecting $\lambda=2.46$ Å. The cryogenic system was the same used for powder diffraction. The sample was a parallelepiped with dimensions $3\times1\times0.5$ mm^3, whose edges were parallel to the pseudocubic unit cell axes. The crystal was twinned forming layers perpendicular to the longest direction so that each layer has one of the four cube diagonals as trigonal axis of the true rhombohedral structure. The crystal was attached to the mixing chamber of the ^{3}He/^{4}He dilution cryostat by a copper plate of about 0.5-mm thick, 0.5-cm wide, and 5-cm long. It was bent at the middle by 45° in order to keep the $[01\bar{1}]_C$ direction upright. This enables us to measure the $(hkk)_C$ reflections. Due to twinning the intensity of such a reflection, recorded by a single detector, is in fact the contribution of four kinds of twins. The angular degrees of freedom were the angle 2θ between the incident and diffracted beams and the rotation angle $0°<\omega<200°$ of the whole cryostat around the vertical axis. Small rotations of the full cryostat around two horizontal axes were allowed in order to center reflections. Optical alignment of the crystal with respect to the rotation axes of the goniometer was performed at room temperature (RT), prior to installing the thermal shielding for the cryogenic device.

This kind of experiment presents some evident advantages over diffraction on powder: the ratio of diffracted intensity to background is much higher and also reflections coming from the sample holder and cryostat can be avoided performing a ω scan (keeping the position of the detector and turning the full device around a vertical axis). In addition to this, the sample holder guarantees a better thermal homogeneity and contact with the mixing chamber than for powder, which can be an essential condition for the present experiment. There are also some drawbacks when working at very low temperatures: only a very limited number of reflections can be measured; the relative values of the intensity of several reflections are not very precise because of the absorption by components of the sample environment; the extinction cannot be corrected properly, the optical alignment of the crystal is not possible, etc. Moreover, in this case the crystal is twinned and usually each diffraction peak is composed of several reflections coming from the different partners, and it is not always possible to assure which one produces each peak or how many of them contribute to the whole intensity.

A check at RT of some nuclear reflections gave typical differences of about 25% between Friedel opposite reflections, which gives an idea of the poor precision in the absolute intensity measurement. By contrast, measurements of the same reflection after several reorientations of the device were reproduced within 1%. Therefore the absolute intensity of a reflection is only an estimation, but its thermal evolution can be considered as very reliable. Typical relaxation times to thermal equilibrium were about 15 min at the lowest temperature reached (49 mK).

The experiment was carried out as follows.

(a) With a view to distinguish the possible ordering modes, or to discard the wrong possibilities, a collection of 32 reflections geometrically accessible and indexable with integer or half-odd numbers with respect to the pseudocubic unit cell was measured. The experiment was performed at 1.035 K (referred to in the following as ''1 K'' data), and at 0.8 K. The aim was to identify the change in intensity of some reflections due to the magnetic ordering below 0.93 K.

(b) We performed systematic $\omega-2\theta$ and ω scans of all magnetic reflections found in (a) from 49 mK up to 0.88 K to study the HENP. The ω scans with 2θ fixed were intended to reveal effects coming from the sample environment, and to correct for the effects of any polycrystalline material disturbing the measurements.

At 1 K all standard nuclear reflections allowed by the space group $R\bar{3}c$ were observed. Most of these are allowed for a perfect cubic perovskite structure and indexable with integer numbers with respect to the pseudocubic axes (substructure reflections). Four observed reflections have half-odd indices (superstructure reflections), namely, $(\pm\frac{1}{2},\frac{3}{2},\frac{3}{2})_C$ and $(-\frac{3}{2},\pm\frac{1}{2},\pm\frac{1}{2})_C$. They are consistent with the kind of distorted perovskite structure described above, and characterized by having three half-odd indices, and at least two of them of different absolute value.[14,15] In this experiment it means that $|h|\neq|k|$, because $k=l$ for the accessible reflections. Due to the twinning of the crystal, some observed superstructure reflections, which are forbidden by the space group $R\bar{3}c$, but allowed for other differently oriented twin partners, are observed. The intensities correspond roughly to the calculated values using the structure factors deduced from the reported atomic positions[9] with the assumption of random distribution of twins. Nevertheless, the reliability factor defined as $R_I=\Sigma(I_{obs}-I_{calc})/I_{obs}\cong0.3$, while in usual four-circles diffractometry the typical values are less than 0.1. This gives also an estimate of the absolute accuracy of the intensity measurement.

Two new reflections appeared in the collection measured at 0.8 K, namely, the $(-\frac{1}{2},\frac{1}{2},\frac{1}{2})_C$ and $(-\frac{1}{2},-\frac{1}{2},-\frac{1}{2})_C$. In addition, the four superstructure reflections, already present

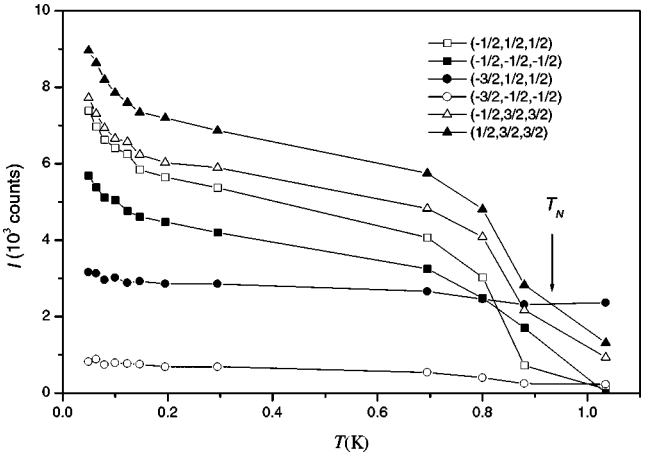

FIG. 3. Thermal evolution of the diffracted intensity of the magnetic lines for the twinned crystal of $NdAlO_3$, showing the HENP below 200 mK. Lines are guides to the eye. The vertical arrow indicates the temperature of antiferromagnetic order $T_N=0.93$ K.

at 1 K, increased their intensity indicating the presence of an antiferromagnetic order.

The evolution of the intensity of the magnetic reflections with temperature is shown in Fig. 3. The increase of the intensities below 200 mK is evident, revealing the HENP effect. In agreement with neutron diffraction, the C_p data[11] did not reveal any Schottky contribution which could be related to the hyperfine polarization above 200 mK in $NdAlO_3$, contrarily to other compounds of the $NdMO_3$ series. It is remarkable that for $NdFeO_3$, with a similar value of m,[6] the magnetic reflection (100) increased already below 500 mK. For $NdCrO_3$, with $m=(1.93\pm0.3)\mu_B$,[16] the hyperfine polarization can be observed already below 1 K in the C_p data.[8]

IV. THE HENP IN $NdAlO_3$

For experiments performed with unpolarized neutrons, each reflection is composed of two contributions which add incoherently: a conventional purely nuclear part and a magnetic plus hyperfine one. For the multidomain single crystal the intensity is given in the Appendix by the rather complicated expression (A7), or by the (A9) expression for a multidomain twinned crystal, with

$$A=\alpha_m f(q), \tag{1}$$

$$B=-\frac{\langle I_z\rangle b_{Nd,inc}}{m\sqrt{I(I+1)}}=-\frac{b_{Nd,inc}I}{m\sqrt{I(I+1)}}B_I\left(\frac{Ig_N\mu_N B_{hf}}{k_BT}\right), \tag{2}$$

where $\alpha_m=\gamma\mu_0 e^2/(8\pi m_e)=2.695$ fm/μ_B is the magnetic scattering length, γ the magnetogyric ratio for the neutron, m_e and e the electron mass and charge, $\mu_0=4\pi\times10^{-7}$ T m/A the vacuum permeability, $f(q)$ the Nd^{3+} magnetic form factor for a given scattering vector $\mathbf{q}$, k_B the Boltzmann constant, $\mu_N=5.0508\times10^{-27}$ J/T the nuclear magneton, m the electronic magnetic moment, g_N the nuclear magnetogyric ratio, and T the absolute temperature. b_{inc} and I are the incoherent scattering length and nuclear spin, respectively, for a particular isotope of the Nd element. $B_I(u)$ is the Brillouin function that describes the nuclear magnetization or the average angular momentum of a nucleus in an external field B_{hf}, in this case produced by the magnetic hyperfine interaction with the electronic moment.

The argument of the Brillouin function is $u=0.5$ for a typical value of the hyperfine field $B_{hf}=100$ T, as encountered in other similar compounds, at 79 mK for ^{143}Nd and at 49 mK for ^{145}Nd. Therefore for $T>80$ mK, $\langle I_z\rangle$ can be approximated by the well-known Curie law:

$$\langle I_z\rangle=\frac{(I+1)u}{3}=\frac{I(I+1)g_N\mu_N B_{hf}}{3k_BT}. \tag{3}$$

This approximation enables to average over the known abundance of the isotopes ^{143}Nd and ^{145}Nd in natural Nd, to give an effective hyperfine scattering length

$$b_{eff}=-\frac{\sqrt{7}}{2}[0.1218\ \ b_{inc}^{143}g_N^{143}+0.0829\ \ b_{inc}^{145}g_N^{145}]$$
$$=(1.33\pm0.18)\text{fm}. \tag{4}$$

In Ref. 6 a factor of 4 was included in b_{eff} to compute the structure factor for four atoms per unit cell. In the present case this factor must be 1 when comparing the intensity with substructure nuclear reflections, indexed with respect to pseudocubic axes, or 6 when referred to hexagonal axes. Substituting in Eq. (2), b_{eff} for $b_{Nd,inc}$ and replacing $\langle I_z\rangle$ by its high-temperature approximation [Eq. (3)]

$$B=b_{eff}\frac{\mu_N B_{hf}}{mk_BT}, \tag{5}$$

which gives $B=0.47$ fm/μ_B for typical values $m=1$ μ_B, $B_{hf}=100$ T, and at $T=100$ mK, whereas A is slightly lower than α_m (i.e., $B/A\sim0.17$). Therefore in the temperature range of interest the term B^2 in the expansion of $(A+B)^2$ in Eq. (A7), or in Eq. (A9), can be dropped out, and the diffracted intensity (I_{diff}) becomes simply proportional to $A+2B$,

$$I_{diff}=C(A+2B)=C\left(\alpha_m f(q)+\frac{\mu_N B_{hf}}{mk_BT}\right), \tag{6}$$

where C is independent of temperature, but different for each reflection. This result holds for powder as well as for a single, multidomain, or twinned crystal. At temperatures well below T_N, when m can be considered independent of T, I_{diff} is proportional to $x=1/T$, and extrapolates to $I_{diff}=0$ for $A=-2B$, that is when

$$x=x_0\equiv-\frac{\alpha_m f(q)mk_B}{2b_{eff}\mu_N B_{hf}}, \tag{7}$$

where all parameters are known, except B_{hf}. Figure 4 shows the intensity of the magnetic reflections versus the inverse temperature. The nuclear part, measured at 1 K, has been subtracted from the experimental intensity. All six reflections show a linear dependence below 300 mK down to 65 mK. The form factors for the reflections $(\pm\frac{1}{2},\pm\frac{1}{2},\pm\frac{1}{2})_C$, $(\pm\frac{3}{2},\pm\frac{1}{2},\pm\frac{1}{2})_C$, and $(\pm\frac{1}{2},\pm\frac{3}{2},\pm\frac{3}{2})_C$ are $f(q)=0.903$, 0.700,

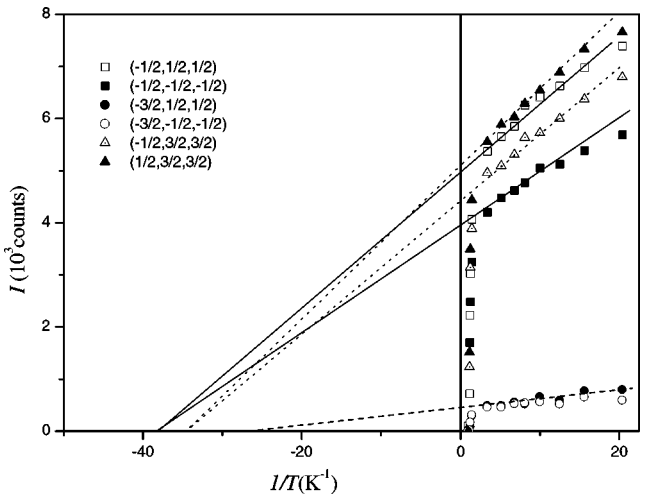

FIG. 4. Plot of the intensity of the observed magnetic lines measured on the crystal of $NdAlO_3$ vs the inverse temperature. The standard nuclear intensity has been measured at 1.035 K and subtracted from the data to get the magnetic plus hyperfine contribution. The straight lines are fits in the temperature range where the dependence is approximately linear, as described in the main text. The vertical line corresponds to $x=0$, or $T\rightarrow\infty$.

and 0.552, respectively.[1] Accordingly, the extrapolations to $I_{diff}=0$ in Fig. 4 should keep the ratio of the form factors. This indeed holds approximately for the four most intense reflections, whereas $(-\frac{3}{2},\pm\frac{1}{2},\pm\frac{1}{2})_C$ are too weak for the extrapolation to give a well-defined result. The magnetic form factor for neutron diffraction is the Fourier transform of the density of the unpaired electrons having magnetic moment. Usually it is computed in the approximation of spherical symmetry (i.e., in the International Tables for Crystallography). Nevertheless this approximation does not necessarily apply to the present compounds. In addition to the experimental problems discussed before, probably the lack of spherical symmetry has a noticeable influence on the anomalous intensities of the high-angle magnetic Bragg reflections for a crystal. The safest procedure is to consider only the $(-\frac{1}{2},\pm\frac{1}{2},\pm\frac{1}{2})_C$ reflections, which are less affected by the form factor, close to unity whatever is the spatial distribution of the electronic magnetic density. The extrapolation to zero gives $x_0=38\mathrm{K}^{-1}$ or $B_{hf}/m=(66\pm5)\mathrm{T}/\mu_B$. Using the value of m obtained from the powder experiment gives $B_{hf}=66\pm10$ T.

The pure magnetic intensity can be obtained extrapolating linearly I_{diff} to $x=0$ $(T\rightarrow\infty)$. The magnetic moment can then be deduced comparing this magnetic intensity with those of pure nuclear reflections, although there are some experimental difficulties that will be discussed below. For the measured magnetic reflections let us define the reduced magnetic intensity as the experimental intensity divided by the Lorentz factor times the squared form factor $[I_{red}=I_{diff}\sin 2\theta/f(q)^2]$ which should be proportional to the trigonometric factor in Eq. (A7) for a single crystal, divided in magnetic domains. Assuming a planar magnetic structure, $\sin^2\theta_m=1$, $\cos^2\theta_m=0$, and this factor reduces to $(1-\frac{1}{2}\sin^2\chi)$, which in turn becomes constant when all twins are equally present in the sample. Under these conditions we expect the same I_{red} for all reflections. It is surprising to find the strong reduced intensity of the $(\pm\frac{1}{2},\frac{3}{2},\frac{3}{2})_C$ reflections and the weakness of the $(-\frac{3}{2},\pm\frac{1}{2},\pm\frac{1}{2})_C$ ones. Nevertheless, the vicinity of the (200) reflection of Cu $(2\theta=86°)$, from the much more massive sample holder, makes the result suspicious even when the data have been subtracted from those at 1 K. We also performed an ω scan with fixed 2θ value to the maximum obtained in the $\omega-2\theta$ scan to avoid the spurious contributions coming from polycrystalline components of the experimental device, but it gave similar results.

The linear extrapolations to $T\rightarrow\infty$ of the magnetic plus hyperfine contribution of the reduced intensities are given in Table I. These results rule out the possibility that all kind of twins and all the domains in each one are equally present. However, there are more unknowns than experimental data if we try to fit the occupancies of all twins and magnetic domains, therefore the direction of the magnetic moment cannot be unambiguously determined. Two simple cases have been tested. For a planar magnetic structure with all domains equally present, the trigonometric factors are also given in Table I. The calculations would be roughly consistent with the experimental data if only the twin 2 (which has the $[\bar{1}11]_C$ as trigonal axis) is present, but this is hardly accept-

TABLE I. Reduced magnetic intensity for the magnetic reflections observed in the twinned crystal, defined as the extrapolation to $T\rightarrow\infty$ of the experimental diffracted intensity minus the nuclear part (measured at 1 K), and divided by the Lorentz $(1/\sin 2\theta)$ and squared magnetic form $[f(q)^2]$ factors. Also the values of $1-(\frac{3}{2}\sin^2\theta_m-1)\sin^2\chi_i\cos^2\theta_m, i=1-4$ [Eq. (A7)] are listed for the four kinds of twins when the magnetic moment is perpendicular to trigonal axis, $\cos\theta_m=0$. The trigonal axis for each twin i is TW1 $\rightarrow[111]_C$, TW2$\rightarrow[1\bar{1}\bar{1}]_C$, TW3$\rightarrow[\bar{1}\bar{1}1]_C$, TW4$\rightarrow[\bar{1}\bar{1}1]_C$.

$(h$	k	$l)_C$	I_{obs}	I_{red}	TW1	TW2	TW3	TW4
$-\frac{1}{2}$	$\frac{1}{2}$	$\frac{1}{2}$	5060	3359	0.56	1	0.56	0.56
$-\frac{1}{2}$	$-\frac{1}{2}$	$-\frac{1}{2}$	3940	2614	1	0.56	0.56	0.56
$-\frac{3}{2}$	$\frac{1}{2}$	$\frac{1}{2}$	443	826	0.52	0.88	0.64	0.64
$-\frac{3}{2}$	$-\frac{1}{2}$	$-\frac{1}{2}$	386	720	0.88	0.52	0.64	0.64
$\frac{1}{2}$	$\frac{3}{2}$	$\frac{3}{2}$	3575	11730	0.72	0.93	0.51	0.51
$-\frac{1}{2}$	$\frac{3}{2}$	$\frac{3}{2}$	2259	7412	0.93	0.72	0.51	0.51

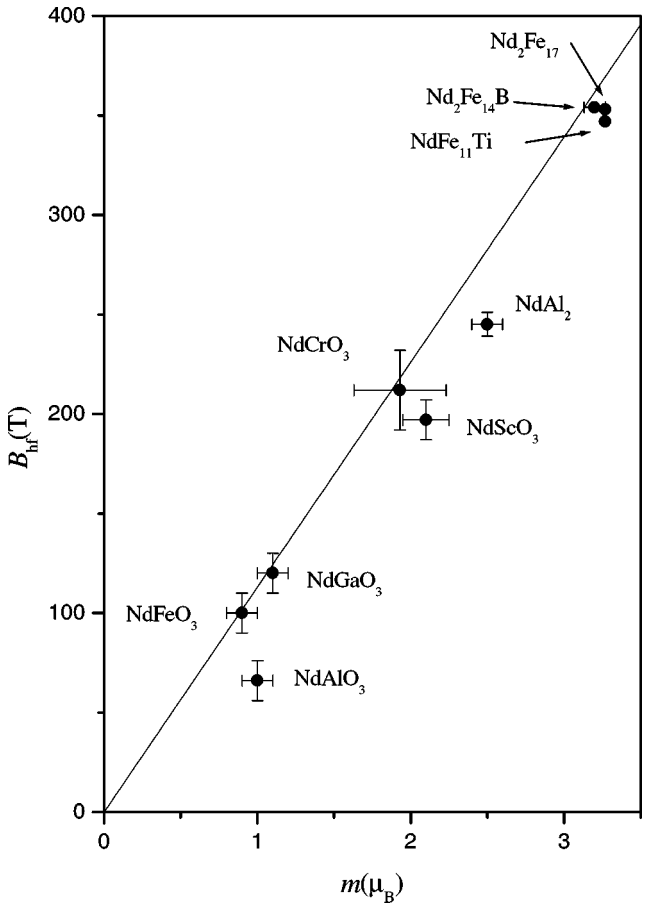

FIG. 5. Plot of hyperfine field vs magnetic moment for several perovskites, with different magnetic moment values. The straight line is the theoretical prediction B_{hf} (T) $=113m(\mu_B)$.

able and incompatible with the experimental fact that at 1 K reflections coming from at least two kinds of twins are observed. Another approach is to assume that all magnetic moments are collinear in the whole crystal, then the direction which agrees the best with the experimental intensities is the $[110]_C$, again consistent with a planar structure. We conclude that the simplest magnetic structure compatible with the experimental data is antiferromagnetic with moments along the $[110]_C$ and perpendicular to the trigonal axis.

The value of the magnetic moment could be obtained if the magnetic intensities can be brought to an absolute scale. However the experimental nuclear intensities agree poorly with the calculated values and the scale factor is estimated with a large standard deviation. Therefore we prefer to take in what follows the value obtained from powder diffraction: $m=(1.0\pm0.1)\mu_B$.

V. STUDY OF THE HENP IN OTHER PEROVSKITES

In this section, we briefly review previous experimental results that provide information on the HENP in several Nd perovskites. We have analyzed the existing data, which are plotted in Fig. 5, using the same method discussed in the preceding section.

$NdFeO_3$ was extensively studied in the past.[6] The data of hyperfine field and magnetic moment are included in Fig. 5. On powder samples the HENP was not observed,[17] probably due to lack of thermal contact between the mixing chamber and sample, the actual temperatures being much higher than the nominal values, as measured at the mixing chamber. The LT magnetic structure of the Nd sublattice is driven by the exchange field with the Fe ions.[6] It can be classified as type $c_y f_x$. Usually the hyperfine contribution to the scattering amplitude is coherently added to that of the magnetic scattering (see the Appendix). The HENP is produced then by the cross terms between these two contributions. The magnetic structure of $NdFeO_3$ has the peculiarity of having a few reflections, allowed by the spatial periodicity of the magnetic lattice but whose usual magnetic diffraction amplitude vanishes because the Nd magnetic moment (m) is parallel to the scattering vector. Thus it was possible to study the hyperfine contribution alone on a single crystal. The pure hyperfine contribution for the reflection (010) and the magnetic plus hyperfine ones for the (100) reflection could be fitted as a function of temperature using only the hyperfine field as parameter, and adjusting the magnetic moment value by comparison with pure nuclear reflections.

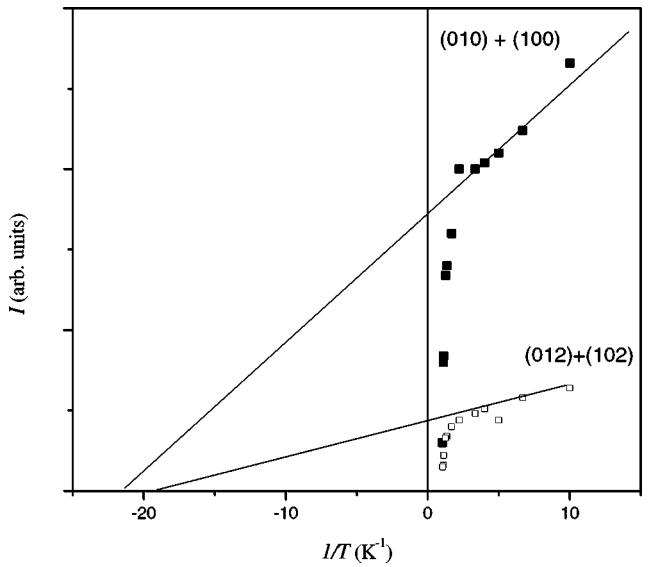

FIG. 6. Plot of the diffracted intensity against $1/T$ for the magnetic reflections (010) + (100) and (012) +(102), of $NdGaO_3$, taken from Fig. 2 in Ref. 2.

For $NdGaO_3$ the data have been taken from Fig. 2 in Ref. 2 and plotted in Fig. 6 as a function of $1/T$. Using expression (7), $B_{hf}/m=110\pm10$ T$/\mu_B$. Taking the magnetic moment obtained in the same work $m=(1.1\pm0.2)\mu_B$ gives $B_{hf}=120$ T.

For $NdScO_3$ the data have been taken from Ref. 5. The ratio B_{hf}/m has been calculated again using expression (7) in order to compare several compounds using the same procedure, rather than the procedure used in the original work, that used the slope of the plot, and where any error on the scale factor affects the result. Finally, $B_{hf}/m=96\pm10$T$/\mu_B, m=2.07(13)\mu_B$, and $B_{hf}=197\pm10$ T.

The compounds $NdCoO_3$ and $NdInO_3$ were studied by neutron diffraction above 250 mK and 280 mK,

respectively,[18] and no indication for HENP was detected. This suggests a lower hyperfine field ($B_{hf}<150$ T). This is very surprising for the In compound since it has the same crystal and magnetic structures and somewhat higher magnetic moment than $NdScO_3$. Thus a similar or stronger hyperfine field is expected. We suggest, as a possible explanation, that the temperature of the sample was higher than the indication of the thermometer attached to the mixing chamber in all experiments performed on powder.

VI. DISCUSSION

We first discuss the type of magnetic ordering in $NdAlO_3$. In the case of distorted perovskites belonging to the orthorhombic space group $Pbnm$ the three nonequivalent directions allow different values of the exchange constants, which can be positive or negative between nearest Nd neighbors in the crystal direction c or in the ab plane, giving a variety of magnetic ordering types in the studied compounds. In $NdAlO_3$, the three pseudocubic cell directions are equivalent by the space-group symmetry $R\bar{3}c$. That is, all Nd-Nd nearest neighbor intervectors and atomic environment are equivalent. Therefore the exchange constants should be equal by symmetry in the three spatial directions, forming a three-dimensional (3D) magnetic lattice.

However, the temperature dependence of C_p data[11] shows a large tail for $T>T_N$, which suggests a low-dimensional magnetic order. Specially the low critical entropy obtained from these data, $S_c/R=0.31(1)$, is quite smaller than the predictions for all simple 3D models of magnetic interaction, but fits very well the theoretical value for 2D Ising models: for the square planar lattice $S_c/R=0.3065$, and for the triangular lattice $S_c/R=0.3303$. This fact is difficult to understand.

A 2D system could occur if the exchange constants between nearest neighbors were very weakly antiferromagnetic and the second neighbor interaction were stronger and ferromagnetic. The second neighbors form planes perpendicular to trigonal axis of the structure. In each plane the Nd atoms form a triangular lattice, with an O atom exactly on the line between each of the two Nd atoms, not equidistant of both. The nearest distance between Nd atoms belonging to consecutive planes (nearest neighbors in the 3D lattice and located at the center of two consecutive pseudocubes) is about $\sqrt{2}$ times shorter but there are no atoms directly in between. This interaction has to be mediated by four O atoms with Nd-O-Nd angles near 90° which could be antiferromagnetic and weaker than the intraplanar interaction. The distance to the next plane is the same as the intraplanar one, but the Nd-O-Nd angle is 168°, which eventually could make the interaction weaker than within a plane. In such a case the system could exhibit a 2D behavior, in agreement with the C_p data.

Now the hyperfine polarization in the perovskites will be discussed. The hyperfine field obtained from the HENP has been plotted against the electronic magnetic moment in Fig. 5. For the orthorhombic perovskites and some other intermetallic compounds the data lie roughly on the straight line $B=Km$ with $K=108$ T/μ_B. This hyperfine polarization has been also observed in LT C_p measurements.[6,8,11,19] The nuclear contribution to the specific heat is related to the thermal population of the nuclear magnetic states, split by the hyperfine field. If $g_N\mu_N B_{hf}/k_BT\ll 1$ holds, this contribution can be written as

$$C_{hf}/R=\frac{I(I+1)}{3}\left(\frac{g\mu_N B_{hf}}{k_BT}\right)^2. \tag{8}$$

Most of the experiments have been performed above 200 mK. As a result, the data provide only a rough estimate of B_{hf}, and only when it is strong enough, $B_{hf}>200$ T. For the Fe, Ga, Co, and Al compounds it has not been observed, in agreement with neutron diffraction data that indicate for them $B_{hf}\approx 100$ T. As an exception the Cr compound is one of the best studied because there are no other distinguishable contributions below 1 K. The hyperfine field (210 ± 20 T) lies on the straight line. For other compounds the C_p data predict hyperfine fields different from the neutron-diffraction results or away from the line, but they have to be taken with skepticism due to experimental difficulties. Therefore one can conclude that in the orthorhombic perovskites the hyperfine field is proportional to the magnetic moment. By contrast, in $NdAlO_3$ the HENP becomes observable unambiguously at lower temperatures than for other perovskites with similar Nd magnetic moment, such as the Fe or Ga compounds. It departs from the straight line to a lower value.

We may compare these results to the expected values from a simple theory. In the rare-earth compounds the crystal field is very weak and splits the ground manifold of the free ion, $^4I_{9/2}$ into five doublets. The coefficients of the ground doublet depend on the symmetry and distances to the neighboring ions and vary from one particular compound to another, resulting in a different magnetic moment. In Nd^{3+} the quadrupolar term of the hyperfine interaction can be neglected against the magnetic term. The magnetic hyperfine field created by the electronic cloud and acting on the nucleus is given by expression (17.32) in Ref. 20, adapted to the International System of Units (IS),

$$\mathbf{B}_{hf}=-2\frac{\mu_0}{4\pi}\mu_B\langle r^{-3}\rangle\mathbf{N}, \tag{9}$$

where the vector **N** is defined in the expression (17.48) of the same reference as

$$\mathbf{N}=\sum_{felectrons}\left\{\mathbf{l}_i-\mathbf{s}_i+3\frac{\mathbf{r}_i\cdot\mathbf{s}_i}{r_i^2}\mathbf{r}_i\right\}, \tag{10}$$

where the core polarization due to s electrons has been neglected, since it is known to account for a few percent at most in $4f$ ions (Table 5.5 and p. 705 in Ref. 20). Usually a precise knowledge of B_{hf} by ENDOR or atomic beam triple resonance is used to determine $\langle r^{-3}\rangle$, allowing a comparison with theoretical atomic models. The ground level of the free Nd^{3+} ion is a linear combination of states with different values of L and S but can approximately be considered as a manifold with $^4I_{9/2}$, since the modulus of the coefficient in the combination exceeds 0.98 (1 means a pure L,S,J state) for $L=6$, $S=3/2$, $J=9/2$.[21] In the ground level of the free

ion characterized by (L,S,J), **N** can be replaced by its projection over **J**, $\langle J\|N\|J\rangle \mathbf{J}$. The reduced matrix element for Nd^{3+} is given in Table 20 of Ref. 20: $\langle J\|N\|J\rangle = 2^2 \times 7 \times 17/(3\times 11^2)$.

The interaction with the crystal field splits the ground ionic level (formed by ten states) into five Kramers doublets. Below T_N, the ground doublet is in turn split by the exchange interactions and the ground single state can be written as a linear combination of the $|JM\rangle$ states with $J=9/2$: $|\Psi_0\rangle = \Sigma_{M=-9/2}^{9/2} C_M |M\rangle$. Then the expected value of the vector **N** is

$$\langle N\rangle = \langle N_z\rangle = \langle J\|N\|J\rangle \sum_{M=-9/2}^{9/2} M|C_M|^2. \tag{11}$$

Moreover the magnetic moment is $\mathbf{m} = -g_J \mu_B \mathbf{J}$ for the free ion with the Landé factor for Nd^{3+} $g_J = 8/11$, which gives the saturation moment $m/\mu_B = g_J J = 36/11 = 3.27$. For the ion in the crystal field the magnetic moment in its ground state is

$$\langle m\rangle = -g_J \mu_B \sum_{M=-9/2}^{9/2} M|C_M|^2 = -g_J \mu_B \frac{\langle N\rangle}{\langle J\|N\|J\rangle}. \tag{12}$$

Therefore the hyperfine field is proportional to the magnetic moment. The ratio is

$$K \equiv \frac{\langle B_{hf}\rangle}{\langle m\rangle} = \frac{\mu_0}{4\pi} \frac{2\langle r^{-3}\rangle}{g_J} \langle J\|N\|J\rangle, \tag{13}$$

when B_{hf} is expressed in tesla, the magnetic moment in Bohr magnetons, and r in atomic units, which makes $K(T/\mu_B) = 22.57\langle r^{-3}\rangle$. For the free ion values of $\langle r^{-3}\rangle \simeq 5$ a.u. are reported,[22] giving $K = 113 \mathrm{T}/\mu_B$, which agrees very well with the experimental values found for well-studied intermetallic compounds with transition-metal atoms as Nd_2Fe_{17}, $NdFe_{11}Ti$ (Ref. 23) where B_{hf} has been determined by NMR or $Nd_2Fe_{14}B$, using ^{145}Nd-Mössbauer spectroscopy.[24]

In other compounds probably $\langle r^{-3}\rangle$ is not too different since the $4f$ electrons are weakly perturbed by the crystal field. Then the ratio of hyperfine field to magnetic moment is expected to be close to the theoretical straight line, as happens with $NdFeO_3$, $NdGaO_3$, and $NdCrO_3$. On the other hand, $NdScO_3$ and $NdAl_2$ fall somewhat below the predicted line (Fig. 5). The experimental point of $NdAlO_3$ falls still lower than both the predicted line and the two latter compounds. Since the Nd^{3+} moment $m = \pm 1\ \mu_B$ is quite similar to that found in the orthorhombic perovskites and to the value deduced from the crystal-field calculations, we believe that this value is beyond doubt. We must conclude that the low value of the hyperfine field we observe is due to an additional opposite contribution to the electronic magnetic-field one. Since the main difference of $NdAlO_3$ to the other perovskites reviewed is the magnetic structure, apparently 2D, and the value of the exchange interaction, we can only conjecture that the exchange biased core-polarization contribution to the hyperfine field is not negligible when compared to the low value in $NdAlO_3$, and is different in the two types of perovskites, giving rise to the departure from the prediction based on the neglect of this contribution.

In summary, the experiments reported in this work reveal some specific features of $NdAlO_3$ when compared with other Nd pseudoperovskites.

(a) The neutron diffraction technique at very low temperatures ($T < 1$ K) allows us to study ordered Nd sublattices in perovskites. Since their magnetic moments differ markedly from the free ion value our experiments have allowed to determine their hyperfine field B_{hf} and find their correlation with the electronic magnetic moment m in a very large range. The analysis of the experimental data shows a linear dependence with $B_{hf}/m = 108\ \mathrm{T}/\mu_B$, very close to the value calculated from simple considerations.

(b) The magnetic structure is a pure antiferromagnetic one, which can be classified as $l = m_1 - m_2$, in the notation of Turov[25] for the space group $R\bar{3}c$, i.e., with antiparallel moments at the two sites of the rombohedral primitive unit cell, and also with all nearest neighbors oppositely oriented. This is in contrast to the $NdMO_3$ orthorhombic perovskites where the pure antiferromagnetic g structure is never found.

(c) The Nd^{3+} magnetic moment is similar to the one found in the orthorhombic perovskites with short Nd-O distances, as in the cases of $NdFeO_3$ or $NdGaO_3$, but the ratio of hyperfine field to magnetic moment is somewhat lower.

ACKNOWLEDGMENTS

The crystal was kindly provided by Dr. M. Marezio from the collection of crystals of late J.P. Remeika. This work was supported by the Spanish research projects MAT02/166 and MAT2001-3507.

APPENDIX HYPERFINE PLUS MAGNETIC STRUCTURE FACTOR FOR A TWINNED CRYSTAL

The magnetic plus hyperfine structure factor is given by the vector[6]

$$\mathbf{F}_{hkl}^{m+h} = \sum_j \exp\left(-B_j \frac{\sin^2\theta}{\lambda^2}\right) \exp[2\pi i(hx_j + ky_j + lz_j)] \times \left(\alpha_m f(q)\langle \mathbf{m}_{j\perp}\rangle - \frac{b_{Nd,inc}\langle \mathbf{I}_j\rangle}{\sqrt{I(I+1)}}\right), \tag{A1}$$

where the summation runs over the Nd atoms in the unit cell, $\alpha_m = 2.695\times 10^{-15}$ m/μ_B is the magnetic scattering length, μ_B the Bohr magneton, $f(q)$ the magnetic form factor, B_j the thermal factor for the atom j, $\mathbf{I}_j$ the nuclear spin operator, $\mathbf{m}_j$ the magnetic moment, $\mathbf{q} = 2\pi(h\mathbf{a}^*, k\mathbf{b}^*, l\mathbf{c}^*)$ the scattering vector, $\mathbf{m}_{j\perp} = \mathbf{m}_j - (\mathbf{m}_j \cdot \mathbf{q})\mathbf{q}/q^2$ the projection of $\mathbf{m}_j$ over the plane perpendicular to **q**, and $b_{\mathrm{Nd},inc}$ the incoherent scattering length of the Nd atom at the site j, at room temperature for thermal neutrons. Only the spin incoherence must be considered: when there are several isotopes a properly weighted average should be made. The angular brackets hold for thermal or quantum average and they will be omitted in the following, when there is no possible confusion.

The thermal parameters B_j are negligible in the range of temperatures of interest in this work. For $NdAlO_3$ the mag-

netic lattice contains two antiparallel moments per primitive rhombohedral unit cell, the positional factors being $+1$ and -1, respectively (multiplied by a physically meaningless global phase which depends on the choice of the coordinate origin), and contributing equally to $\mathbf{F}_{hkl}$ for the allowed reflections, which can be indexed with respect to the pseudocubic unit cell with all the three half-odd numbers. Therefore only one atom needs to be considered. Moreover, due to the strong hyperfine field the nuclear spin has the same direction as the magnetic moment. Then the structure factor can be written as

$$\mathbf{F}=A\mathbf{m}_{\perp}+B\mathbf{m}=(A+B)\mathbf{m}-A\frac{\mathbf{m}\cdot\mathbf{q}}{q2}\mathbf{q}, \tag{A2}$$

where $A=\alpha_m f(q)$ and $B=-\langle I\rangle b_{\mathrm{Nd},inc}\langle m\rangle\sqrt{I(I+1)}$. For a single crystal the diffracted intensity is proportional to

$$|\mathbf{F}|^2=(A+B)^2m^2-(A^2+2AB)\frac{(\mathbf{m}\cdot\mathbf{q})^2}{q^2}. \tag{A3}$$

In the range of temperatures of interest usually $B\ll A$ holds and $(A+B)^2$ can be replaced by A^2+2AB, which results for $|\mathbf{F}|^2$ an expression similar to the usual magnetic diffraction, replacing $A+B$ for A. In this case the cross term $2AB$ dominates the additional contribution due to the hyperfine polarization of the nuclear spins. Nevertheless, when $\mathbf{q}$ is parallel to $\mathbf{m}$, $\mathbf{m}_{\perp}=0$, and the pure hyperfine contribution is then proportional to m^2B^2, giving a quite weaker extra contribution, as seen in $NdFeO_3$, Ref. 6.

In a crystal belonging to the $R\bar{3}c$ space group, there are six equivalent directions to a given one. Half of them are related by the threefold symmetry axis and the other half are related to the former one by a glide symmetry plane (the generator c in the space group symbol, which acts as a pure binary axis on the magnetic moments). When the crystal orders antiferromagnetically, if the easy direction is without a special symmetry, it splits into six kinds of magnetic domains. Three of them are related by successive 120° rotations around the trigonal axis. The remaining three by the c glide plane. There can also be domains related by pure translation or inversion of the sense of the moments, and separated by 180° domain walls, but these are not distinguishable by neutron diffraction. Let us call $\mathbf{m}_e$ the projection of the magnetic moment on the trigonal axis and $\mathbf{m}_p$ the projection on the plane perpendicular to it. The scattering vector $\mathbf{q}$, which is perpendicular to the family of crystallographic planes (hkl) and has a modulus $q=4\pi\sin\theta/\lambda$, can also be decomposed into two perpendicular vectors $\mathbf{q}_e$ and $\mathbf{q}_p$. The squared scalar product in Eq. (A3) can be written as

$$\begin{aligned}(\mathbf{m}\cdot\mathbf{q})^2&=(\mathbf{m}_p\cdot\mathbf{q}_p+m_eq_e)^2\\&=(\mathbf{m}_p\cdot\mathbf{q}_p)^2+(m_eq_e)^2+2\mathbf{m}_p\cdot\mathbf{q}_pm_eq_e.\end{aligned} \tag{A4}$$

Let us call φ the angle between m_p and q_p, χ the angle between $\mathbf{q}$ and the trigonal axis, and θ_m the angle between $\mathbf{m}$ and the trigonal axis. Let us assume that there is the same volume of each kind of domains. Then the square of the structure factor for a single domain must be replaced by the average of three terms with φ, $\varphi+120°$, and $\varphi-120°$, respectively. The product m_eq_e is the same for all three, while the average of $\mathbf{m}_p\cdot\mathbf{q}_p$ vanishes and the average of its square is

$$\langle(\mathbf{m}_p\cdot\mathbf{q}_p)^2\rangle=\frac{1}{3}\sum_{n=0,\pm1}\left[m_pq_p\cos\left(\varphi+\frac{2\pi n}{3}\right)\right]^2=\frac{1}{2}m_p^2q_p^2. \tag{A5}$$

The same result holds for the three domains related by the c glide plane. The average of $(\mathbf{m}\cdot\mathbf{q})^2$ can be obtained by substituting Eq. (A5) in Eq. (A4):

$$\begin{aligned}\frac{\langle(\mathbf{m}\cdot\mathbf{q})^2\rangle}{m^2q^2}&=\frac{1}{m^2q^2}\left(\frac{1}{2}m_p^2q_p^2+m_e^2q_e^2\right)\\&=\left(\frac{3}{2}\sin^2\theta_m-1\right)\sin^2\chi+\cos^2\theta_m.\end{aligned} \tag{A6}$$

The diffracted intensity is proportional to the average of the squared magnetic plus hyperfine structure factor of a single domain, obtained by inserting Eq. (A6) into Eq. (A3):

$$\begin{aligned}\langle|\mathbf{F}|^2\rangle=m^2\{&(A+B)^2-(A^2+2AB)\\&\times[(\tfrac{3}{2}\sin^2\theta_m-1)\sin^2\chi+\cos^2\theta_m]\}.\end{aligned} \tag{A7}$$

Therefore, when $B=0$, that is, for a pure magnetic case, this expression reduces to the usual diffracted intensity for a multidomain crystal, while when the nuclear polarization is sizable, it gives rise to a term proportional to A^2+2AB (which adds coherently to the magnetic contribution) and to another which adds incoherently to the magnetic part, proportional to B^2, which is independent of the direction of $\mathbf{q}$ and $\mathbf{m}$.

In the present case the crystal is twinned, the trigonal axis being one of the four ternary axes present in a perfect cubic perovskite structure, namely, the directions $[111]_C$, $[\bar{1}11]_C$, $[\bar{1}\bar{1}1]_C$, and $[1\bar{1}1]_C$, which can be obtained by successive 90° rotations around one of the fourfold axes of the cube. Let us denote these directions by the vector $\mathbf{e}=(e_x,e_y,e_z)$, with $e_i=\pm1, i=x,y,z$. In this work the hexagonal axes are taken as sketched in Fig. 1, that is, the indexation is strictly correct for the twin that has the $[111]_C$ as trigonal axis, or nominal twin. For a particular reflection $\mathbf{q}$ has any direction. Its components with respect to the cubic axes are denoted by $\mathbf{q}=(q_x,q_y,q_z)$. The angle χ with the trigonal axis of a particular twin is given by

$$\cos\chi=\frac{\mathbf{e}\cdot\mathbf{q}}{eq}=\frac{e_xq_x+e_yq_y+e_zq_z}{q\sqrt{3}}. \tag{A8}$$

The sum of the squared cosines for the four kinds of twins is $\Sigma_{i=1}^4\cos^2\chi_i=4/3$. When all the four kinds of twins are equally present, the intensity of a reflection produced by the magnetic plus hyperfine polarization is obtained by replacing in Eq. (A7) $\sin^2\chi$ by $\frac{1}{4}\Sigma_{i=1}^4\sin^2\chi_i=2/3$, to get the average squared structure factor for a multi-domain twinned crystal or a powder:

$$\langle|\mathbf{F}^{m+h}|^2\rangle = m^2\{(A+B)^2-(A^2+2AB)[(\tfrac{3}{2}\sin^2\theta_m-1)^{\frac{2}{3}} + \cos^2\theta_m]\} = m^2[\tfrac{2}{3}(A+B)^2+\tfrac{1}{3}B^2]. \quad \text{(A9)}$$

Therefore, on a powder or a multidomain twinned crystal, when the reflections coming from a single domain or twin cannot be resolved, 2/3 of the amplitude of the hyperfine contribution adds coherently to the usual magnetic one, and 1/3 of the hyperfine part does incoherently, irrespectively of the direction of **m** or **q**. At not too low temperatures usually $B \ll A$, and the cross term $4AB/3$ in the expansion of $2(A+B)^2/3$ dominates the hyperfine contribution. It can be computed simply by adding the hyperfine amplitude B to the magnetic one A, and neglecting the term $B^2/3$.

On a powder, if the rhombohedral distortion is enough to resolve the Bragg peaks, then the intensity is given by expression (A7) times the multiplicity, scale, and Lorentz factors because each crystallite can have the magnetic moment in any of the equivalent easy directions. For the reflection $(1/2,1/2,1/2)_C=(003)_H$, $\sin^2\chi=0$. For $(1/2,-1/2,1/2)_C=(0\bar{1}1)_H$, in an undistorted cubic structure, $\sin^2\chi=8/9$. Using the crystallographic data of Ref. 9, $\sin^2\chi=a^{*2}/(a^{*2}+c^{*2})=0.8870$.

*Author to whom correspondence should be addressed. FAX: 34-76761229; electronic address: elias@posta.unizar.es

[1] *International Tables for Crystallography*, edited by A.J.C. Wilson (Kluwer, Dordrecht, 1992), Vol. C.

[2] W. Marti, M. Medarde, S. Rosenkranz, P. Fischer, A. Furrer, and C. Klemenz, Phys. Rev. B **52**, 4275 (1995).

[3] O. Elsenhans, P. Fischer, A. Furrer, K.N. Clausen, H.G. Purwins, and F. Hulliger, Z. Phys. B: Condens. Matter **82**, 61 (1991).

[4] T. Chattopadhyay and K. Siemensmeyer, Europhys. Lett. **29**, 579 (1995).

[5] I. Plaza, E. Palacios, J. Bartolomé, S. Rosenkranz, C. Ritter, and A. Furrer, Physica B **234-6**, 635 (1997).

[6] J. Bartolomé, E. Palacios, M.D. Kuz'min, F. Bartolomé, I. Sosnowska, R. Przeniosło, R. Sonntag, and M.M. Lukina, Phys. Rev. B **55**, 11 432 (1997).

[7] E.F. Bertaut, *Spin Configurations of Ionic Structures: Theory and Practice in Magnetism*, edited by G.T. Rado and H. Suhl (Academic Press, New York, 1963), Vol. III, p. 149.

[8] F. Bartolomé, J. Bartolomé, M. Castro, and J.J. Melero, Phys. Rev. B **62**, 1058 (2000).

[9] M. Marezio, P.D. Dernier, and J.P. Remeika, J. Solid State Chem. **4**, 11 (1971).

[10] C.J. Howard, B.J. Kennedy, and B.C. Chakoumakos, J. Phys.: Condens. Matter **31**, 349 (2000).

[11] F. Bartolomé, J. Bartolomé, and J. Blasco, J. Magn. Magn. Mater. **157–158**, 491 (1996).

[12] *Neutron-Scattering Instrumentation at the Research Reactor BER II*, edited by the Berlin Neutron Scattering Center of the Hahn-Meitner-Institut (http://www.hmi.de), Berlin, 1996.

[13] E. Antic-Fidancev, M. Lemaitre-Blaise, L. Beaury, G. Teste de Sagey, and P. Caro, J. Chem. Phys. **73**, 4613 (1980).

[14] A.M. Glazer, Acta Crystallogr., Sect. A: Cryst. Phys., Diffr., Theor. Gen. Crystallogr. **A31**, 756 (1975).

[15] K.S. Aleksandrov, Ferroelectrics **14**, 801 (1976).

[16] N. Shamir, H. Shaked, and S. Shtrikman, Phys. Rev. B **24**, 6642 (1981).

[17] R. Przeniosło, I. Sosnowska, P. Fischer, W. Marti, F. Bartolomé, J. Bartolomé, E. Palacios, and R. Sonntag, J. Magn. Magn. Mater. **160**, 370 (1996).

[18] I. Plaza, E. Palacios, J. Bartolomé, S. Rosenkranz, C. Ritter, and A. Furrer, Physica B **234-6**, 632 (1997).

[19] F. Bartolomé, J. Bartolomé, and R.S. Eccleston, J. Appl. Phys. **87**, 7052 (2000).

[20] A. Abragam and B. Bleaney, *Electron Paramagnetic Resonance of Transition Ions* (Dover, New York, 1986).

[21] B.G. Wybourne, J. Chem. Phys. **34**, 279 (1961).

[22] K.F. Smith and P.J. Unsworth, Proc. Phys. Soc. **86**, 1249 (1965).

[23] C. Kapusta and P.C. Riedi, in *NMR Studies of Intermetallics and Interstitial Solutions Containing H, C, and N*, Vol. 281 of *NATO Advanced Study Institute, Series E: Applied Sciences*, edited by F. Grandjean, G.L. Long, and K.H.J. Buschow (Kluwer, Dordrecht, 1995), Chap. 20.

[24] I. Nowik, K. Muraleedharan, G. Wortmann, B. Perscheid, G. Kaindl, and N.C. Koon, Solid State Commun. **76**, 967 (1990).

[25] E.A. Turov, *Physical Properties of Magnetically Ordered Crystals* (Academic Press, New York, 1965), Chap. V.